

Z0 Resonance

Santiago Rodriguez, Birge Sükrü Tok

¹*Institut of Physics, Humboldt University Berlin, Germany*

Instructor: R D Parsons

(Experiment Date: 8.2.2021, Report Date: 25.2.2021)

Datasets on e^+e^- reactions from the L3 experiment at CERNs LEP accelerator are reprocessed in order to compute the cross section σ of said reactions, the characteristic constants of the Z0 boson M_Z, τ_Z of its mass and lifetime, as well as the weak mixing angle Θ_W corresponding to the Weinberg angle in the theory of the electroweak interaction. From the evaluation of the datasets, values of $M_Z = (91.2 \pm 0.04)GeV, \Gamma_Z = (2.59 \pm 0.07)GeV, \tau_Z = (2.48 \pm 0.1) \cdot 10^{-25}s$ and $\sin^2 \Theta_W = \{0.22 \pm 0.01, 0.28 \pm 0.01\}$ were computed and remain consistent with the predictions made using the standard model of particle physics.

I Introduction and Theory

During e^+e^- interactions, neutral current interactions mediated by the Z boson -the messenger particle responsible for the weak force alongside the W^+ and W^- bosons- provide a mechanism for the annihilation of the e^+e^- pair into fermions $f = q, e, \mu, \tau, \nu$ and their respective antifermions \bar{f} by means of the reaction $e^+e^- \rightarrow Z_0 \rightarrow f\bar{f}$. These neutral currents of Z bosons were first theorized as a way to describe the elastic scattering of neutrinos with other particles $\mu N \rightarrow Z_0 \rightarrow \mu N$ in the standard model. Without them, scattering processes like the conversion of neutrinos to W bosons $\nu_\mu + \bar{\nu}_\mu \rightarrow W^+W^-$ would break the unitarity limit by means of the proportionality to E^2 of their cross sections $\frac{d\sigma}{d\Omega} \simeq s = (p_\nu = p_{\bar{\nu}})^2 = E_{CM}^2$. For it to work within the established quantum mechanical laws, an additional step $\nu_\mu + \bar{\nu}_\mu \rightarrow Z_0 \rightarrow W^+W^-$ needs to be defined such that the cross section $\frac{d\sigma}{d\Omega} \approx s \rightarrow \infty \frac{1}{s}$ compensates for it -the additional step being the Z boson.

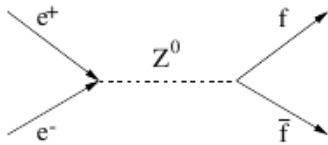


Figure 1: Production and decay of a Z_0 boson during a e^+e^- annihilation [1]

Depending on their energy, e^+e^- pairs can decay into fermion and antifermion pairs either via QCD by exchanging a photon if their center-of-mass energy \sqrt{s} is far below the energy threshold $\sqrt{s} \ll M_Z$ for the production of Z_0 bosons, or on the contrary annihilate primarily through the Z_0 channel if $\sqrt{s} \sim M_Z$, at which point the Z_0 resonance dominates during the production of further fermions. In this case, the characteristic values for the Z_0 boson, namely its cross section σ_Z mass M_Z and lifetime τ_Z , can be extracted from the different events produced by e^+e^- annihilations. In addition, the weak mixing angle Θ_W -or Weinberg angle as it is also called- which describes the relation between the mass of the Z and W bosons, can also be determined. For this experiment, the analyzed data includes decays into both hadrons from the resulting $e^+e^- \rightarrow Z_0 \rightarrow q\bar{q}$ as well as muons $e^+e^- \rightarrow Z_0 \rightarrow \mu^+\mu^-$.

II L3 Setup

The L3 detector was one of 4 main Detectors at the former LEP (Large Electron Positron Collider) at CERN. LEP was shut down on November 2. to make way for the construction of the LHC (Large Hadron Colider) and thus L3 was replaced by the ALICE (A Large Ion Collider Experiment) experiment. [8] The data used in this analysis originates from this detector.

L3 was designed to study e^-e^+ collisions at energies of up to 200 GeV, however this potential was not fully realized, as the highest energy beam created in the LEP was of 104,5GeV in May 2000. For our purposes, collisions at around 90 GeV are relevant.

L3 housed a multitude of sub detectors, in order to detect and measure various particles and their decays. Starting from the center, the first subdetectors are the Vertex chamber and Time Expansion Chamber, which measure the trajectory of charged particles. This is followed by the electromagnetic calorimeter (also known as BGO as it is made of Bismuth Germanium Oxide) measuring the energy of leptons, along with the hadron calorimeter measuring the energy of hadrons. Calorimeters are made of dense materials, and stop most particles, thus releasing and measuring their energy. Finally, the muon chambers, where muons are detected, are located between the hadron calorimeter and the Magnet coils, which generate a magnetic field within the detector, which in turn enables energy measurements of particles through their deflection. All of these detectors are placed concentrically, in the form of cylinders, around the collision chamber, which is capped by luminosity monitors measuring the luminosity of the incoming beams.

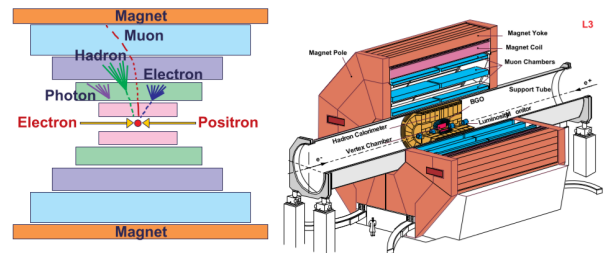


Figure 2: Schematic of the L3 experiment[4]

This order is preferable, as heavier and more en-

ergetic particles, muons, require more material than the calorimeters provide to be stopped and thus detected. Ergo the placement of the muon chambers as last detectors was chosen. Similarly, the electromagnetic calorimeter is exposed to the particle fallout before the hadron calorimeter, as electrons and positrons for example are more likely to be detected here, and hadrons more likely to pass. Finally, the scintillators are placed between the calorimeters, as it is expected, that close to none of the gamma rays generated in the collision may pass beyond this point. This is to filter out gamma ray events caused by high energy cosmic rays which otherwise may interfere with measurements.

III Selection of Hadron and Muon Events

III.1 Hadronic Events

The selected hadronic events were chosen based on three criteria; first, the total calorimetric energy of the selected hadrons needed to be around the same value of the center-of-mass energy \sqrt{s} . With an energy of

$$E_{Vis} = \sum_{i=1}^n E_i = \sum_{i=1}^n \sqrt{\vec{p}_i^2 + m_i^2} \approx \sum_{i=1}^n \sqrt{p_{xi}^2 + p_{yi}^2 + p_{zi}^2} \quad (1)$$

for a total of n particles, the following relation for the ratio must hold true

$$0.5 < \frac{E_{Vis}}{\sqrt{s}} < 1.5 \quad (2)$$

as according to [3]. According to the same source, the energy imbalances along the beam direction ΔE_{\parallel} and perpendicular to it ΔE_{\perp} as given by the formulas

$$\Delta E_{\perp} = \sqrt{\left(\sum_{i=1}^n p_{xi}\right)^2 + \left(\sum_{i=1}^n p_{yi}\right)^2} \quad (3)$$

$$\Delta E_{\parallel} = \sum_{i=1}^n p_{zi} \quad (4)$$

need to also stay within a range of

$$|\Delta E_{\parallel}|/E_{Vis} < 0.6 \quad (5)$$

$$\Delta E_{\perp}/E_{Vis} < 0.5 \quad (6)$$

in order to be qualified as valid hadronic events from a Z decay process.

III.2 Muon Events

For the selected muon events, three different criteria were also chosen. First, as according to [3], the muon event must be within the angular range

$$0 < |\cos(\Theta)| < 0.8 \quad (7)$$

with

$$\cos(\Theta) = \frac{p_z}{\sqrt{p_x^2 + p_y^2 + p_z^2}} \quad (8)$$

Then, their energy in the form of their momentum $E_{mu} \approx \sqrt{p_{xi}^2 + p_{yi}^2 + p_{zi}^2}$ should be roughly $1/2\sqrt{s}$ since most of the beam energy is conserved and thus

$$40GeV \leq E_{mu} \approx \sqrt{p_{xi}^2 + p_{yi}^2 + p_{zi}^2} \leq 50GeV \quad (9)$$

In addition, the total impulse of both muons must lie below 5GeV since their opposite directions due to energy conservation would make their total impulse add up to 0.

$$p_{tot} = \sqrt{\vec{p}_{\mu} + \vec{p}_{\bar{\mu}}} \leq 5G \quad (10)$$

III.3 Systemic deviation

The events selected according to these criteria for an experimental set of data are compared to the data from Monte-Carlo simulations in the figure below.

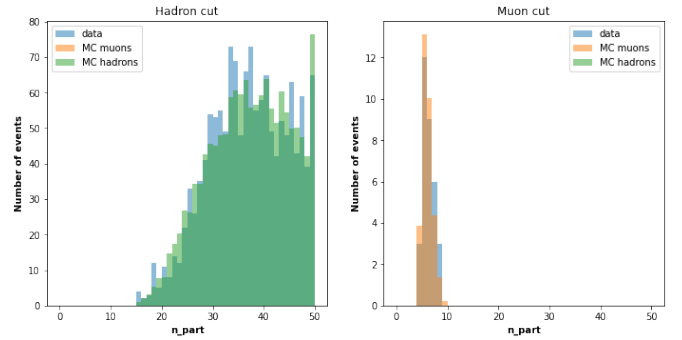


Figure 3: Data Cuts compared with the MC data

The efficiency ϵ of the cuts can be calculated according to the formula

$$\epsilon = \frac{N'_{MC}}{N_{MC}} \quad (11)$$

where N'_{MC} is the number of selected events in the Monte-Carlo simulation used as a sample for the selection algorithm and N_{MC} is the total number of events.

$\frac{E_{vis}}{\sqrt{s}}$	$\frac{ \Delta E_{\parallel} }{E_{vis}}$	$\frac{\Delta E_{\perp}}{E_{vis}}$	89GeV	91GeV	93GeV
$0.5 << 1.5$	< 0.6	< 0.5	1780	3984	2127
$0.6 << 1.4$	< 0.5	< 0.4	1762	3928	2096
$0.4 << 1.6$	< 0.7	< 0.6	1790	4010	2141

Table 1: Data selection with different criterias for Hadrons

In order to determine the systemic uncertainties of the hadron and muon events selection algorithms, some of the cuts were varied in order to check on the variation in selected events and estimate a systemic uncertainty from them. For hadron cuts, this uncertainty was roughly ascertained to be around $u_{hadr} \approx 25$ and for muons $u_{mu} \approx 7$ by looking at the rough distribution between numbers of selected events.

IV Cross Sections of Hadron and Muon Events

For calculating the cross sections of the hadrons and muons, the selected hadron and muon events are evaluated together with the efficiency ϵ (11) of the selection, acceptance A of the detector and the luminosity \mathcal{L} of the beams arriving at the detector. These luminosities are given (see Table 5) for each dataset with a relative uncertainty of 1%.

$\sqrt{s}(\text{GeV})$	$\mathcal{L}(\text{nb}^{-1})$
89,48	179,3
91.33	135,9
93,02	151,1

Table 2: Given Luminosities of datasets by energy

The cross sections are yielded using the following relation

$$\sigma = \frac{N_{obs}}{\epsilon A \mathcal{L}} \quad (12)$$

where N_{obs} is the number of observed events.

However, as efficiency and acceptance are calculated through an extrapolation from data generated using a Monte-Carlo simulation, (12) may be simplified as follows;

$$\sigma = \frac{N' - N^B}{\epsilon \mathcal{L}} \quad (13)$$

Here N' is the number of events and N^B the estimated number of background events, after the application of criteria from III. By applying a Gaussian propagation of , the uncertainty for the computed cross sections σ becomes

$$u_\sigma = \sqrt{\sum_{i=1}^m \left(\frac{\partial y}{\partial x_i} \cdot u_i \right)^2} \quad (14)$$

$$\sqrt{\left(\frac{1}{\epsilon \mathcal{L}} \cdot u_{N'} \right)^2 + \left(\frac{1}{\epsilon \mathcal{L}} \cdot u_{N^B} \right)^2 + \left(\frac{N' - N^B}{\epsilon^2 \mathcal{L}} \cdot u_\epsilon \right)^2 + \left(\frac{N' - N^B}{\epsilon \mathcal{L}^2} \cdot u_{\mathcal{L}} \right)^2} \quad (15)$$

Due to the strong agreement between the Monte Carlo datasets seen in figure 3 and the selected experimental data, a background signal N^B can be neglected without compromising the results from the computations. Thus, both $N^B = 0$ and $u_{N^B} = 0$ are set a priori for the next steps. This then yields the following values for the cross sections of hadrons and muons with the uncertainties u_σ

$\sqrt{s}(\text{GeV})$	$\mathcal{L}(\text{nb}^{-1})$	$\sigma_{hadr}(\text{nb})$	$\sigma_\mu(\text{nb})$
89,48	179,3	10 ± 0.6	0.4 ± 0.03
91.33	135,9	$29,4 \pm 0.8$	1.18 ± 0.03
93,02	151,1	$14,2 \pm 0.7$	0.46 ± 0.03

Table 3: Cross sections for Hadrons and Muons

V Breit Wiegner Fit

The cross section distribution $\sigma(s)$ as a function of the square of the center-of-mass energy \sqrt{s} for both the

hadron and muon events takes the form of a Breit-Wigner curve as expressed by the formula

$$\sigma(s) = \sigma_0 \cdot \frac{s\Gamma_Z^2}{(s - M_Z^2)^2 + M_Z^2\Gamma_Z^2} \quad (16)$$

In order to fit this model function to the data, a non linear fit to the convolution integral

$$\sigma^{corr}(s) = \int_0^s \sigma(s') \cdot r(s, s') ds' \quad (17)$$

is conducted by means of a least-squares method where for the previously computed σ_i with $i \in \{1, 2, 3\}$ and the fitted $\sigma^{corr}(s)$ the expression

$$\chi^2 = \sum_{i=1}^3 \frac{(\sigma_i(s) - \sigma^{corr}(s))^2}{u_\sigma^2} \quad (18)$$

becomes minimal. The convolution integral corrects the Breit-Wiegner model with a function $r(s, s')$ for the probability of a photon emission, in which case the squared center-of-mass energy s would be reduced from s to $s' < s$. From this model, the fitted parameters $\sigma_0 =, M_z =, \Gamma_z =$ giving the characteristic values of the Z boson can be determined. Running this fitting algorithm for the cross sections computed above, the Breit-Wiegner fit for hadron events follows below.

V.1 Hadron Cross Sections

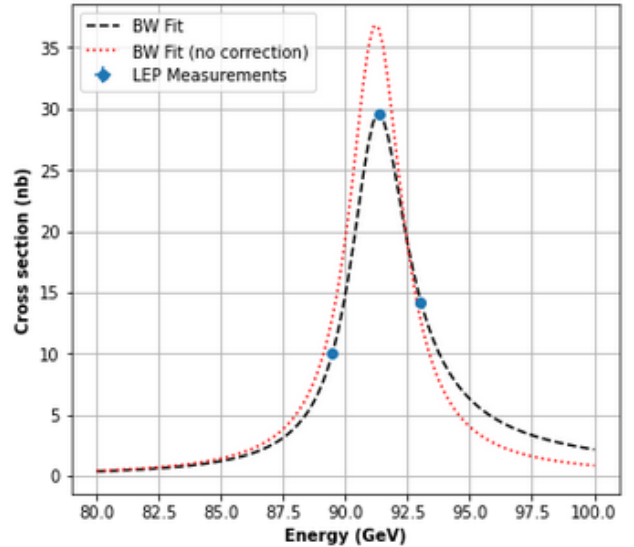


Figure 4: Breit Wigner Fit for Hadrons

The dotted red figure shows the fit without corrections, while the black one compensates for the energy loss discussed above. From the plot, a good agreement between the model and the data can already be observed, with the following characteristic parameters of the Z resonance

Parameter	Value
σ_0	$(36.9 \pm 0.6) \text{nb}$
M_Z	$(91.2 \pm 0.04) \text{GeV}$
$ \Gamma_Z $	$(2.59 \pm 0.07) \text{GeV}$

Table 4: Parameters computed from the Breit-Wigner Hadron Fit

V.2 Muon Cross Sections

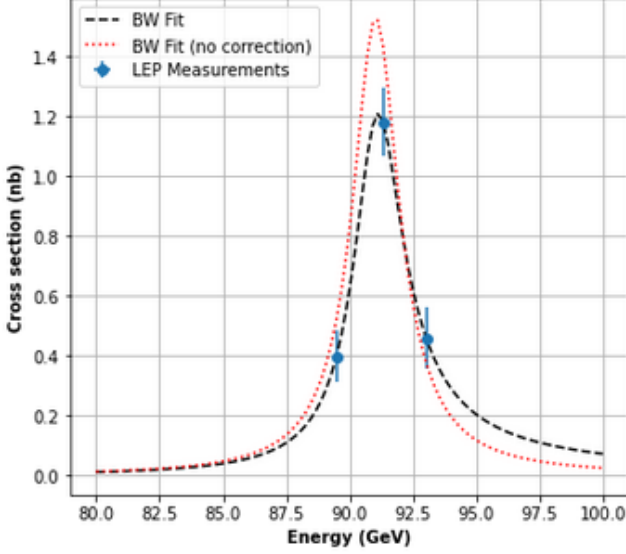


Figure 5: Breit Wigner Fit for Muons

The same fit can then also be computed for the selected muon events and computed cross sections σ_{mu} , yielding the figure above. For it, the fitted parameters are returned as

Parameter	Value
σ_0	$(1.5 \pm 0.6)nb$
M_Z	$(91 \pm 0.8)GeV$
$ \Gamma_Z $	$(2.3 \pm 1.4)GeV$

Table 5: Parameters computed from the Breit Wigner Muon Fit

where both the mass M_Z and partial width Γ_Z of the Z boson for the hadron and muon fits overlap very well, with the parameters determined by the hadron fit yielding a lower uncertainty than the ones from the muon fits. Lastly, the lifetime τ_Z of the Z boson can be computed from the inverse value of the decay width Γ_Z as according to

$$\tau_Z = \frac{1}{\Gamma_Z} = 0.38 \pm 0.01 GeV^{-1} \cdot 6.582 \cdot 10^{-25} s / GeV^{-1} \quad (19)$$

$$\tau_Z = 2.48 \pm 0.1 \cdot 10^{-25} s \quad (20)$$

VI Partial Width of Electron Γ_e

VI.1 From Muon Cross Section

The partial width of the electrons Γ_e can also be inferred through the characteristic fitted parameters for the Z boson, either through the muon or the hadron data. In the former case, the relationship between the maximum value of the cross section $max(\sigma(s)) = \sigma_0$, which is given as

$$\sigma_0 = \frac{12\pi}{M_Z^2} \cdot \frac{\Gamma_e \Gamma_f}{\Gamma_Z} \quad (21)$$

can be utilized for events where the resulting particle is a fermion such as a muon $f = \mu$ such that $\Gamma_f = \Gamma_\mu$.

Since according to the universality of leptonic decays the relation $\Gamma_l = \Gamma_\tau = \Gamma_e = \Gamma_\mu$ holds true, the formula could be simplified for $\Gamma_e = \Gamma_\mu$ as follows

$$\sigma_0^{mu} = \frac{12\pi}{M_Z^2} \cdot \frac{\Gamma_e \Gamma_\mu}{\Gamma_Z} = \frac{12\pi}{M_Z^2} \cdot \frac{\Gamma_e^2}{\Gamma_Z} \quad (22)$$

Thus, solving for Γ_e delivers

$$\Gamma_e = M_Z \Gamma_Z \sqrt{\frac{\sigma_0}{12\pi}} \quad (23)$$

with the uncertainties resulting from Gaussian error propagation being

$$u_{\Gamma_e} = \sqrt{(T_Z \sqrt{\frac{\sigma_0}{12\pi}} \cdot u_{M_Z})^2 + (M_Z \sqrt{\frac{\sigma_0}{12\pi}} \cdot u_{T_Z})^2 + (M_Z T_Z \sqrt{\frac{12\pi}{\sigma_0}} \cdot \frac{u_{\sigma_0}}{2})^2} \quad (24)$$

and thus the resulting value for the partial width as calculated using the muon cross section being

$$\Gamma_e = (76 \pm 6) MeV \quad (25)$$

There is another way to determine the partial width too however, by using the hadron cross sections.

VI.2 From Hadron Cross Section

As the total width of the Z-Resonance may be obtained through the sum of all partial widths, $\Gamma_e = \Gamma_l$ may be obtained using following relation.

$$\Gamma_Z = \Gamma_{hadron} + 3\Gamma_l + 3\Gamma_{\nu l} \quad (26)$$

Here the factors 3 are obtained through the universality's of leptons and neutrinos.

Furthermore, solving 21 for Γ_f and substituting $f = hadron$, delivers a method of calculating the partial width of hadron decay.

$$\Gamma_{hadron} = \frac{M_Z^2 \sigma_0^{hadron} \Gamma_Z^2}{12\pi \Gamma_e} \quad (27)$$

Substituting 27 into 26, and solving for Γ_e

$$\Gamma_e = \frac{\Gamma_Z/3 - \Gamma_{\nu e}}{2} - \sqrt{\left(\frac{\Gamma_Z/3 - \Gamma_{\nu e}}{2}\right)^2 - 4 \frac{M_Z^2 \sigma \Gamma_Z^2}{36\pi}} \quad (28)$$

leads to a final requirement to solve: $\Gamma_{\nu e}$, which is calculated using following equation and substituting $f = \nu_e$ and $Q_{\nu e} = 0$ as neutrinos are not charged, thus eliminating the need for the Weinberg angle for this calculation.

$$\Gamma_f = \frac{G_F M_Z^3}{24\sqrt{2}\pi} \cdot [1 + (1 - 4|Q_f| \sin^2 \Theta_W)^2] \quad (29)$$

ergo

$$\Gamma_{\nu e} = 2 \frac{G_F M_Z^3}{24\sqrt{2}\pi} \quad (30)$$

Through this method $\Gamma_e = (75.44 \pm 13.28)eV$ was calculated. However, a Gaussian uncertainty propagation failed, due to complex values being attained. More on this topic in the discussion.

VII Weinberg Angle Θ_W

In the standard model, the electroweak mixing angle, also called the Weinberg angle, gives the decay widths of fermions according to 29.

$\sin(\Theta)^2$ can thus be computed by means of the partial width derived above from the muon and hadron events. By rewriting the equation for the Weinberg angle Θ_W , the following expression

$$\sin^2(\Theta_W) = \left(1 \pm \sqrt{\frac{\Gamma_f}{\frac{G_F M_Z^3}{24\sqrt{2}\pi}} - 1} \right) \cdot \frac{1}{4|Q_f|} \quad (31)$$

returns the desired value, with $\Gamma_f = \Gamma_e = (83.35 \pm 0.08)$ being the decay width computed in IX, $G_F = 1.166 \cdot 10^{-5} 1/GeV^2$ the Fermi constant and $M_Z = (91.2 \pm 0.04) GeV$ the mass of the Z boson determined in IV. Since the root within the equation can be positive or negative, two possible values for $\sin\Theta^2$ are given as follows;

$$\sin(\Theta)_1^2 = 0.22 \pm 0.01 \quad \sin(\Theta)_2^2 = 0.28 \pm 0.01 \quad (32)$$

VIII Quark Colors

In order to determine the amount of quark colors N_C , first the cross section Γ_{hadr} needs to be determined. This cross section follows from the relationship between the decay width of the Z boson the rest of the decay widths adding up to it

$$\Gamma_Z = \Gamma_{hadr} + 3\Gamma_\nu + 3\Gamma_l \quad (33)$$

where there is three components to the lepton and neutrino decay width due to universality meaning all neutrino flavors also sharing the same decay width. $\Gamma_l = \Gamma_e$ is already known and Γ_ν can be computed through

$$T_\nu = \frac{G_F M_Z^3}{12\sqrt{2}\pi} = (0.165 \pm 0.1) GeV \quad (34)$$

since neutrinos are electrically neutral and so $Q_f = Q_\nu = 0$. From these known values, the decay width of the hadrons follows as

$$\Gamma_{hadr} = \Gamma_Z - 3\Gamma_\nu - 3\Gamma_l = (1.86 \pm 0.1) GeV \quad (35)$$

From this, the color factor NC which quantifies the quark colors can be computed through the formula

$$\Gamma_{hadr} = N_C \cdot K_{QCD} \cdot (2\Gamma_u + \Gamma_d) \quad (36)$$

where the decay widths of the up and down quarks are given for a known Weinberg angle Θ and their charges $Q_u = 2/3$, $Q_d = -1/3$ as

$$\Gamma_d = (0.124 \pm 0.06) GeV \quad \Gamma_u = (0, 097 \pm 0.06) GeV \quad (37)$$

Thus, rewriting for NC and with $K_{QCD} \approx 1.04$ -which is a factor taking into account the possibility of gluons being emitted by the quarks- the color factor NC yields the following value

$$N_C = \frac{\Gamma_{HadR}}{K_{QCD} \cdot (2\Gamma_u + 3\Gamma_d)} \approx (3.2 \pm 0.3) \quad (38)$$

IX Discussion

From the calculations above and results $M_z = (91.2 \pm 0.04) GeV$, $\Gamma_z = (2.59 \pm 0.07) GeV$ and $\sin^2 \Theta_W = \{0.22 \pm 0.01, 0.28 \pm 0.01\}$, the comparison with the literature values [9] $M_Z^{lit} = (91.195 \pm 0.006) GeV$, $\Gamma_z = (2.49 \pm 0.01) GeV$ and $\sin^2 \Theta_W = 0.2283 \pm 0.0032$ yields a favorable verdict on the correct computation of the results above.

Due to a failure of obtaining an uncertainty through a Gaussian uncertainty propagation in VI, the uncertainty of Γ_e attained through hadron data was estimated, by multiplying the sum of the relative uncertainties of the parameters and multiplying this sum by the number of parameters and the value attained. A likely source of this failure lies in the calculation of σ_0^{hadron} , Γ_Z or Γ_{ve} . Attempts to rectify this remained unfruitful.

A better selection of events in order to maximize the efficiency and thus reduce the error of the initially computed cross sections, as well as a more accurate assessment of the uncertainties would have likely provided better results, since the values from literature seem to provide further accuracy on their measurements. In addition, the convergence of the Breit-Wigner fit could have been improved for further center-of-mass energy \sqrt{s} measurements and cross section values $\sigma(s)$ to feed into the fitting algorithm. As it stands, the produced χ^2 are far below any otherwise minimum standards.

But nonetheless, both the measurements as well as the results from the data processing seem to completely remain in agreement with the predictions by the standard model. The applied cuts and criteria on the data were also selectively able to filter out most non-relevant events and keep those already simulated by the Monte-Carlo datasets, confirming the hypothesis even further. Thus the results from the experiment and data processing further support the validity of the standard model in particle physics.

A References

- [1] Kapitel 4 (Neutrale Ströme) der VL Experimentelle Elementarteilchenphysik
- [2] DESY, Von der Z-Entdeckung zu den Z-Fabriken, https://www-zeuthen.desy.de/~husemann/teaching/2009_ss/exp_teilchenphysik/skript/skript_03.pdf last accessed: 22.02.2021
- [3] O. Adrinai et al., Results from the L3 Experiment at LEP, Physics Reports 236(1993)1
- [4] M. zur Nedden, R D Parsons, U. Schwanke, F. Peri; Instructions for the Z0 Praktikum
- [5] M. zur Nedden, U. Schwanke; Anleitung zum Versuch "Z0-Resonanz" im Fortgeschrittenen-Praktikum

- [6] Martin Grunewald, Thomas Hebbeker Teilchenphysik am $e^+ e^-$ Speicherring LEP, Physikalische Blätter 51(1995)837
- [7] H. Schopper, Die Ernte nach einem Jahr LEP-Betrieb, Physikalische Blätter 47(1991)907
- [8] L3|CERN, <https://home.cern/science/experiments/l3>, last accessed: 25.02.2021
- [9] Giulia Pancheri and Yogendra N. Srivastava, Introduction to the physics of the total cross-section at LHC A Review of Data and Models